

RSC Advances



This is an *Accepted Manuscript*, which has been through the Royal Society of Chemistry peer review process and has been accepted for publication.

Accepted Manuscripts are published online shortly after acceptance, before technical editing, formatting and proof reading. Using this free service, authors can make their results available to the community, in citable form, before we publish the edited article. This *Accepted Manuscript* will be replaced by the edited, formatted and paginated article as soon as this is available.

You can find more information about *Accepted Manuscripts* in the [Information for Authors](#).

Please note that technical editing may introduce minor changes to the text and/or graphics, which may alter content. The journal's standard [Terms & Conditions](#) and the [Ethical guidelines](#) still apply. In no event shall the Royal Society of Chemistry be held responsible for any errors or omissions in this *Accepted Manuscript* or any consequences arising from the use of any information it contains.



Journal Name

ARTICLE

Preparation and Characterization of Novel Ag doped Hydroxyapatite-Fe₃O₄-Chitosan hybrid composites and its *In vitro* Biological evaluations for Orthopaedic applications

Received 00th January 20xx,
Accepted 00th January 20xx

DOI: 10.1039/x0xx00000x

www.rsc.org/

U. Anjaneyulu^a, V.K. Swaroop^b and U. Vijayalakshmi^{a*}

This investigation represents the fabrication of novel composites having biopolymer Chitosan with Ag doped Hydroxyapatite (HAP)-Magnetite nanoparticles (Fe₃O₄ NPs). In this study, Ag doped HAP was synthesized by sol-gel method using different silver concentrations such as 1, 3 and 5% respectively. Furthermore, Fe₃O₄ NPs were prepared by co-precipitation technique and the composite was developed with Ag doped HAP. The fabricated Ag:HAP-Fe₃O₄ composites were incorporated into the chitosan matrix by planetary ball milling technique and were tested for its reliability as a promising biomaterial for orthopaedic applications. The present paper aims to evaluate the *in vitro* hemocompatibility of Ag doped HAP-Fe₃O₄ incorporated chitosan composites using hemolytic assay at the concentrations of 200, 400, 600, 800 and 1000 µg/ml. The results have shown that the developed composites exhibit hemolytic ratio of less than 5 %, which proved them as good blood compatible in nature. The antibacterial activity of the composites was evaluated in *Staphylococcus aureus* (*S. aureus*), *Escherichia coli* (*E. coli*) bacteria which determine that the composites can extensively inhibit the active growth of microorganisms. In addition to this, *in vitro* bioactivity behavior was performed in SBF solution for 7 days in order to analyze the carbonated apatite formation on the surfaces of composites and found to have characteristic bone bonding ability. The *in vitro* biocompatibility of the fabricated nanocomposite (C-3) was examined by MTT assay using NIH-3T3 fibroblast cells for an incubation period of 24, 48 h and the exposed concentrations are similar to hemolytic assay. This MTT assay indicates that the fibroblast cells were non toxic up to the concentration of 400 µg/ml with prominent cell attachment, proliferation on C-3 composites. These prepared composite materials were further characterized by ATR-FTIR, powder-XRD and SEM-EDAX analysis. The research findings have shown that the hybrid composites of 5%Ag:HAP-Fe₃O₄-Chitosan can be widely used as a favourable material for orthopaedic and dental applications.

1. Introduction

Synthetic biomaterials such as composites and substituted bioceramic materials play an important role in orthopaedic and dental applications, especially used in large bone defects and heavy load bearing areas. Hydroxyapatite (HAP) is a synthetic bone mineral which is used as a bone graft, drug carrier and as coatings on metal alloys due to its osteoconductivity and biocompatibility.^{1,2} However, its poor antibacterial activity and various bacterial infections can cause severe pain and often results in removal of ceramic bone grafts, which restricts the use of pure HAP in the long term *in vivo* applications.³ To overcome these issues, the use of

antimicrobial agents by doping or substituting metal ions such as Ag⁺, Zn²⁺, Cu²⁺ and Ti⁴⁺ etc in HAP.⁴ Among these, silver (Ag⁺) is a versatile metal ion to minimize the microbial infections owing to its excellent antibacterial ability, thermal stability and biocompatibility.⁵ Ag⁺ at lower concentration is non toxic and at a higher level, it is toxic to the human body, which leads to the argyrosis. Ag doped HAP is mostly used as powder form or as coatings on orthopaedic implants and medical devices because of its exceptional properties such as direct bone bonding ability with human bone, biocompatibility and preventing the adhesion of microorganisms.⁶

Chitosan (CS) is a natural biopolymer which is composed of *N*-acetyl glucosamine, glucosamine residues and deacetylated derivative of chitin.⁷ In the past few decades, CS extremely used in clinical applications such as cosmetics, pharmaceuticals, biomedical field and tissue engineering due to its attractive behaviors of biodegradability, biocompatibility and low toxicity.⁸ Generally, CS with mesoporous silica and HAP composites plays a vital role in improving the mechanical properties for weight bearing bone applications as well as to enhance the osteoconductivity, protein adhesion and osteoblast proliferation than the carbonated apatite.^{9,10}

^aMaterials Chemistry Division, School of Advanced Sciences, VIT University

^bBiomedical Science Division, School of Biosciences and Technology, VIT University Vellore -632014, Tamil Nadu, India.

Tel: +91-416-2202464; Fax: +91-416-224 3092.

E-mail address: vijayalakshmi.u@vit.ac.in, lakesminat@yahoo.com

Iron oxide (Fe_3O_4) NPs are super paramagnetic material and intensively developed as a potential candidate for the biomedical applications such as hyperthermia therapy, drug delivery, biocatalyst, biological separation and magnetic resonance imaging (MRI).¹¹ However, the direct usage of Fe_3O_4 NPs may have long term cytotoxic to the human environment. These nanoparticles can contaminate the blood plasma and leads to hemolytic which may cause death to the normal cells. This problem can be effectively solved by developing composites with bioceramics or biopolymers.¹² Hydroxyapatite and Fe_3O_4 composites are used in the application of cancer treatment like bone tumors due to the magnetically induced heat generation in an alternating magnetic field.¹³ HAP coated on Fe_3O_4 NPs potentially applied in the disease of osteoporosis and promotes the bone growth of the desired bone defect area.¹⁴ Hence, HAP- Fe_3O_4 is an emerging composite material for the tissue engineering applications.

Hemocompatibility is one of the characteristic natures of medical devices and used in contact with human blood. Usually, the interaction of materials with red blood cells (RBC) can cause damage to cells and release the intracellular hemoglobin which termed as hemolytic.¹⁵ Even though, the mechanism involved in this interaction is still unclear¹⁶ and the materials which exhibits the percentage of hemolysis less than 5% indicates the safe use in medical applications.¹⁷ *In vitro* biocompatibility investigations are highly recommended to test the toxicity behavior of ceramics and its nanocomposites with mammalian cells. Therefore, these nanocomposites should not be toxic to bone forming cells for use in tissue engineering applications. P. Jongwattanapisan et al, have prepared hydroxyapatite/chitosan-silica nanocomposite and examined its *in vitro* bioactivity also cytocompatibility with rat osteoblast-like UMR-106 cells, which were proved as a filler material for bone regeneration.¹⁸ W. Cui et al have synthesized a novel three dimensional nanocomposite of HAP/ Fe_3O_4 /CS by *in situ* compositing method and they found that the nanocomposites exhibit superparamagnetic behavior.¹⁹ W. Jia et al, have prepared HAP/ Fe_3O_4 /CS composites using *in situ* compositing method and studied its mechanical properties for the application in bone repair.²⁰

Recently, a great deal of interest has been focused on the preparation of ceramic composite materials to improve the mechanical and biological properties than the individual materials. The composite materials such as HAP-CS^{21,22} and HAP- Fe_3O_4 ^{23,24} were proved as remarkable bone grafts for technological applications. However, to the best of our knowledge, there has been no research report on the preparation of multiphase composite materials with combinations of Ag doped HAP, Fe_3O_4 and CS. In this present investigation, we have carried out the development of hybrid composites using planetary ball milling with three different materials such as Ag doped HAP, Fe_3O_4 and Chitosan which could enhance the bone healing and curing the bone cancer. These hybrid composite materials were assessed for hemolytic test to evaluate compatibility with blood and also antibacterial activity was examined using gram positive (*S. aureus*), gram negative (*E. coli*) pathogens. *In vitro* apatite formation ability of 5%@Ag:HAP- Fe_3O_4 -CS composites were analyzed by

immersion in the simulated body fluid (SBF) solution for 7 days. The biocompatibility study was examined on the nanocomposite (C-3) which cultured with NIH-3T3 cells for 24 and 48 h at 200-1000 $\mu\text{g}/\text{ml}$. The different concentrations Ag doped HAP (1%, 3% & 5%), Fe_3O_4 , CS and their composites were further characterized by valuable techniques such as ATR-FTIR, powder-XRD and SEM-EDS analysis.

2. Materials and Methods

2.1. Materials

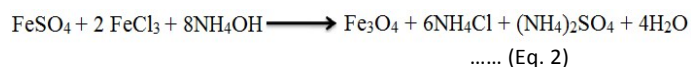
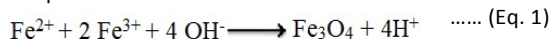
Calcium nitrate ($\text{Ca}(\text{NO}_3)_2 \cdot 4\text{H}_2\text{O}$ SDFCL), Orthophosphoric acid (H_3PO_4 SDFCL-80%), Aq. Ammonia (Aq. NH_3 SDFCL-30%), Silver nitrate (Sigma Aldrich-99%), Iron sulphate (FeSO_4 SDFCL), Iron chloride anhydrous (FeCl_3 SDFCL), Chitosan (Sigma Aldrich) and Phosphate buffer solution (PBS) solution.

2.2. Preparation of Ag doped HAP by Sol-Gel method.

The stoichiometric amount of $\text{Ca}_{10-x} \text{Ag}_x(\text{PO}_4)_6(\text{OH})_2$ with $x=1, 3$ and 5 % were prepared by sol-gel method to maintain the ratio of Ag+Ca/P as 1.67. The calculated amount of calcium nitrate and silver nitrate were added to the double distilled (DD) H_2O . The mixture was stirred for 30 min before addition of aq. NH_3 (pH=10) followed by the addition of orthophosphoric acid. A white precipitate was formed and the pH of the mixture was adjusted to 10 by the addition of aq. NH_3 . The obtained white gel was continuously stirred for 2 h and aged for 24 h at room temperature. The aged mixture was dried at 100 °C for 12 h and washed with DD H_2O for several times to make aq. NH_3 free raw powder. The raw powders were further heat treated at 900 °C for 2 h to obtain the phase pure Ag doped HAP with nano size.

2.3. Synthesis of Fe_3O_4 by Co-Precipitation method

Nano sized Fe_3O_4 was synthesized by co-precipitation method using ferrous and ferric salts, with the molar ratio of 1:2. In this process, initially, 1M of FeSO_4 (5.560g) and 2M of FeCl_3 (6.488g) were added to 100 ml of DD H_2O and the reagents were dissolved using magnetic stirrer for 30 min (pH~2). To this mixture a 15 ml of aq. NH_3 solution was added to uphold a pH of 10, followed by a colour change from light brown to black within an hour at 80 °C. Thus formed Fe_3O_4 NPs were separated by external magnetic field and subjected to repeated wash with DD H_2O , to maintain a neutral pH. The final suspension was rinsed with acetone and dried in an oven at 100 °C for 1h to obtain the Fe_3O_4 NPs. The plausible chemical reactions are mentioned in the equation-1&2.



2.4. Fabrication of hybrid composites of 5%@Ag:HAP- Fe_3O_4 -CS

The calculated weight ratio of 5%@Ag:HAP, Fe_3O_4 and CS powders were mixed homogeneously using agate mortar and pestle for 1 h. The obtained mixture was subjected to ball milling (VB Ceramic consultant) using silicon carbide (SiC) balls with the size of 10 mm diameter. The weight ratio of SiC balls to powder was maintained at 20:1 and the rotation speed was kept at 450 rpm for 2 h to prepare the hybrid composites of 5%@Ag:HAP- Fe_3O_4 -CS. In these composites, the weight % of 5%@Ag:HAP powder was fixed as 50 % and the remaining ratios of Fe_3O_4 NPs and chitosan was altered as 50:45:5 (C-1), 50:35:15 (C-2) and 50:25:25 (C-3) respectively. These hybrid composites were further studied for *in vitro* hemocompatibility and antibacterial activity.

2.5. Antibacterial activity

The antibacterial activity was carried out using human pathogens *S. aureus* (MTT3680) gram positive and *E. coli* (MTT9721) gram negative bacteria. The seed cultures were prepared by inoculating a loop full of culture in 10 ml of autoclaved sterile broth and incubated at 37 °C for overnight. 2 % of the overnight cultures were transferred into a side arm conical flask containing 100 ml of sterile nutrient broth and further incubated at 37 °C in a temperature controlled orbital shaker till the culture has reached 0.5 OD, where un-inoculated broth served as a control.²⁵

The cell pellet was obtained by centrifuging 2 ml of 0.5 OD seed culture at 6000 rpm for 5 min, followed by washing with sterile PBS solution. Further, the culture along with phosphate buffer solution (PBS) was transferred into various falcon tubes each containing different materials i.e. Ag doped HAP, Fe₃O₄, C-1, C-2 and C-3 at a concentration of 5 mg/ml. The inoculated tubes were incubated for 4 h at 37 °C in a temperature controlled incubator. The cultures in the absence of the materials served as a control. After the incubation, these tubes were subjected to the serial dilution, in this 10⁻³ dilution tubes were selected and 0.1 ml of sample was streaked on to the agar plates followed by incubation at 37 °C for overnight. Thus, formed colonies were counted using digital colony counter and the CFU/ml was calculated using following formula.

$$\text{CFU/ml} = \text{No. of colonies} \times \text{Dilution factor} / \text{Volume of culture plate}$$

2.6. In vitro Bioactivity study

Simulated body fluid (SBF) solution was used to evaluate the *in vitro* apatite formation ability due to its ionic concentration is almost similar to the human blood plasma. Therefore, this *in vitro* SBF immersion study usually employed as a pre-requirement of *in vivo* bioactivity assessment. The SBF solution was prepared according to the procedure developed by Kokubo et al.²⁶ using the reagents of NaCl (7.996g), NaHCO₃ (0.350g), KCl (0.224g), K₂HPO₄ (0.228), MgCl₂·6H₂O (0.305g), CaCl₂ (0.278g), Na₂SO₄ (0.071g) and C(CH₂OH)₃NH₂·HCl (6.057g). These reagents are subsequently added to the DD H₂O (1L) and maintained the pH at 7.35±0.25 followed by storing in refrigerator. The 50 mg of prepared composites of 5%Ag:HAP-Fe₃O₄-CS (C-1, C-2&C-3) powders were immersed in the 50 ml of SBF solution for 7 days at 37 °C with subsequent refreshment of solution for every 24 h. After SBF treatment, the composites were analyzed by using SEM-EDAX to determine the deposition of carbonated HAP on the surface.

2.7. In vitro Hemocompatibility test

To assess the hemocompatibility of the prepared materials, fresh blood samples were procured from VIT University health center, from which 5 ml was withdrawn aseptically and centrifuged for 3 min at 10,000 rpm to separate out the plasma from blood cells. The supernatant was discarded and 2 ml of blood was transferred into a falcon tube containing 4 ml of sterile PBS and washed thoroughly. Thus, the obtained mixture was subjected to centrifugation at 10,000 rpm for 15 min at 4 °C. The above step was repeated thrice and the pellet was dissolved in 20 ml of sterilized PBS and maintained at 4 °C. 0.2 ml of blood was taken and mixed with 0.8 ml of PBS containing various concentrations of the 5%Ag:HAP, Fe₃O₄ and hybrid composites in a sterile Eppendorf and incubated for 1 h at 37°C in shaking condition. Upon incubation, the tubes were centrifuged at 10,000 rpm for 3 min and the supernatant solution was collected and readings were taken at 570/655 nm using BIORAD ELISA plate reader in a 96 well micro titer plate. The 0.2 ml of blood and 0.8 ml of water served as positive control, whereas with PBS served as negative control. The hemocompatibility of the composites was determined using the following formula.^{27,28}

$$\text{Hemolytic percentage} = \frac{\text{Sample absorbance} - \text{Negative control}}{\text{Positive control} - \text{Negative control}} \times 100$$

2.8. MTT assay

The 40 % (v/v) dimethylformamide (DMF) in 2 % (v/v) glacial acetic acid followed by the addition of 16 % (wt/v) sodium dodecyl sulfate (SDS) was used as a solvent to dissolve the C-3 composites and makes the final volume concentration of 0.5 % and it did not affect cell survival. The NIH-3T3 cells were maintained at a concentration of 5x10³ cells per well by adding separately in 96 well plates and Dulbeccos Modified Eagle Medium (DMEM-150µl) was added to these wells to grow the cells. After this step, the fibroblast cells were washed with serum free medium (100 µl) for twice and starved for 1 h at 37 °C. After starvation, the NIH-3T3 fibroblast cells were treated with various concentrations of C-3 composites (200, 400, 600, 800 and 1000 µg/ml) for an incubation period of 24 and 48 h. The control was maintained without C-3 composites and at the end of the experiment for each period, the medium was aspirated and serum free medium containing 0.45 mg/ml of MTT (3-[4,5-dimethylthiazol-2-yl] 2,5-diphenyl tetrazolium bromide) reagent was added and incubated for 4 h at 37 °C in CO₂ incubator. These determinations were performed using triplicates each time.

The MTT containing medium was then removed and the NIH-3T3 cells were washed with phosphate buffer solution (PBS-200 µl) to eliminate the unreacted MTT reagent and C-3 composite. The formed formazan crystals were dissolved by adding DMSO (100 µl) and this was mixed thoroughly by pipetting up and down. Spectrophotometrical absorbance of the purple blue formazan dye was measured in a microplate reader at 570 nm (Biorad 680) and cell viability was determined by Graph pad prism 5 software. The viable NIH-3T3 cells were observed by using inverted phase contrast microscopy.

$$\text{Percentage of cell viability} = \text{Sample OD} / \text{Control OD} \times 100$$

2.9. Characterization

Both composites (C-1 to C-3) and Ag doped HAP with 1 to 5% were characterized to identify the functional groups by fourier transform infrared with attenuated total reflectance spectroscopy (ATR-FTIR) in the range of wave number from 4000-400 cm⁻¹ using SHIMADZU model spectrophotometer, for comparison Chitosan was also analyzed. The phase purity along with other composition and crystallinity were examined by using Bruker D8 Advance X-Ray diffractometer, with a step size of 0.02° using Cu Kα (1.5406Å) with Ni filtered radiation and analyzed the data by portable crystal impact match 1.9a software. Surface morphology and chemical composition of individual components and their composites were observed by Scanning electron microscopy-Energy dispersive X-ray spectroscopy (SEM-EDAX:SEM S4800 Hitachi). ICP analysis was used to determine the chemical composition of the SBF immersed composite materials (Perkin Elmer Optima 5300 DV). The amount of silver release from 5%Ag:HAP, C-1, C-2 and C-3 were measured by atomic absorption spectroscopy (AAS-Varian Co. Australia) analysis using phosphate buffer solution. The 5%Ag:HAP and nanocomposite powders were separately dissolved in 1 M of HCl solution and the resultant solution was diluted in 100 ml of DD H₂O. The Ag ions present in the test solutions were measured using AgNO₃ as standard solution in the range of 0.5-3.5 ppm.

3. Results and Discussion

3.1. FT-IR analysis

The ATR-FTIR spectra of Ag doped HAP with concentrations from 1 to 5% were shown in the Fig. S1 (a)-(c). These characteristic

bands clearly represent the vibrational modes of phosphate and hydroxyl groups present in the structure of Ag doped HAP crystal.^{29,30} The reduction in the peak intensities of OH⁻, PO₄³⁻ and CO₃²⁻ moieties indicates the slight alteration of HAP structure and this was further proved by powder-XRD analysis.

The IR spectrum (Fig. 1 (a)) of pure chitosan shows the significant absorption peaks at 1381 and 1315 cm⁻¹ are belong to the bending mode of the methylene C-H and stretching mode of the amide C-N bonds respectively. In this spectrum, very weak bands were observed in the range of 1577-1654 cm⁻¹ which is attributed to the bending vibration of N-H bond in NH₂ group.^{31,32} and the remaining vibrational bands of CS were stated in supplementary information (SI). From Fig. 1 (b) it was found that the presence of broad characteristic absorption band at 536 cm⁻¹ denotes the formation of Fe₃O₄ NPs.³³ The FT-IR spectrum (Fig. 1 (d)-(f)) of composites has shown the characteristic vibrational bands of HAP. It was found that, the broadness of peak width from 560-636 cm⁻¹ was increased compared with 5%Ag:HAP (Fig. 1 (c)) due to the presence of Fe₃O₄ NPs in composites. The peak broadness of C-1 to C-3 decreased with the lower amount of Fe₃O₄ NPs inclusion in the composites. The detailed assignment of bands is listed in SI. These ATR-FTIR characteristic bands confirm that the obtained composite comprises of Ag:HAP, Fe₃O₄ and CS materials.

3.2. Powder-XRD

The XRD pattern of Ag doped HAP (1%, 3% and 5%) powders heat treated at 900 °C for 2 h are shown in Fig. S2 (a)-(c). In these patterns, 1 to 5% of Ag doped HAP samples are completely matches with the standard pattern of HAP (JCPDS#9-432) with hexagonal crystal symmetry and space group of P6₃/m. The most characteristic diffraction peaks with miller indices values of Ag doped HAP has shown in table 1. These peak positions of Ag doped HAP are accordance with the parent pattern of crystalline HAP.^{34,35} The crystallite size ($D=0.9\lambda/\beta\cos\theta$), crystallinity ($\chi_c=0.24A^2/B_{1/2}^3$) and lattice parameters ($1/d^2=4/3[h^2+hk^2+k^2/a^2]+l^2/c^2$ & $V=\sqrt{3}ac^2$) are shown in the table S1.

The XRD pattern (Fig. 2 (a)) of chitosan exhibits a broad diffraction peak at $2\theta=20.10^\circ$ and confirms the presence of phase pure CS with semi crystalline nature.³⁶ Fig. 2 (b) represents the XRD pattern of Fe₃O₄ NPs and confirms the phase pure formation of spinal structured Fe₃O₄ with no other impurities. The characteristic diffraction peaks along with the indices values are represented in table 1, which are found to be consistent with the standard crystal planes of Magnetite NPs (JCPDS#85-1436).³⁷ The broad diffraction peaks determines the size of Fe₃O₄ particles are in the range of 40-95 nm. The XRD patterns comprised of 5%Ag:HAP-Fe₃O₄-CS nanocomposites along with 5%Ag:HAP are shown in the Fig. 2 (c)-(f). The C-1, C-2 and C-3 composites exhibit the significant diffract peaks of Ag:HAP at 25.9-34°, Fe₃O₄ at 30.2-62.8° however, there is no strong peak at 20.1° for CS due to the interference of highly crystalline Ag:HAP phase. However, the XRD spectra of composites are slightly amorphous when compared with the pure phase of 5%Ag:HAP, which proves the accompanying phase of CS. The crystallinity of nanocomposites is increased from C-1 to C-3 due to the decrease in the wt% of Fe₃O₄ in the composites which is correlated with IR spectra of composites. Also the peak intensities of Fe₃O₄ NPs in C-1 to C-3 are slowly reduced and which evidenced for the experimental wt % in composites. These XRD patterns of nanocomposites confirm the presence of Ag:HAP, Fe₃O₄ NPs and CS without any other calcium phosphate phases.

3.3. SEM-EDAX

The surface morphology of 5%Ag:HAP, Fe₃O₄ and CS are represented in the Fig. 3. As observed in SEM micrographs, Ag doped HAP particles (Fig. 3 (a)) are agglomerated and non-

uniform in size. The morphology of the particles resembles an elongated spherical shape with a size of nano to submicron range. Fe₃O₄ NPs (Fig. 3 (b)) are distributed in the range of nano regime with highly dense and agglomerated morphology. CS micrograph (Fig. 3 (c)) reveals the smooth surface sheet like shape with shrinkage manner. The Fig. 3 (d)-(f) illustrates the surface analysis of C-1, C-2 and C-3 nanocomposites after ball milling for 2 h at 450 rpm respectively. The C-1, C-2 and C-3 exhibit the incorporation of Ag:HAP and Fe₃O₄ NPs on the surface of CS matrix. The Ag:HAP and Fe₃O₄ particles are merged together with a reduction in the size, which leads to the increase in the surface area. With the decrease in the wt% of Fe₃O₄ NPs and the increase in the wt % of CS in C-3 composite have shown uniform distribution of particles over CS compare to C-1 and C-2 composites.

From Fig. 3A (a)-(c), the major constituents such as Ca, P, O and Ag are observed in the 5%Ag:HAP with Ca+Ag to P ratio as 1.67, Fe, O for Fe₃O₄ and also the high wt % of C, O in the CS are originated from the long carbon chain of CS matrix. The EDAX analysis (Fig. 3A (d)-(f)) confirms the chemical composition of 5%Ag:HAP-Fe₃O₄-CS composites with presence of Ag, Ca, P, O and Fe elements. From the EDAX study of composite materials such as C-1, C-2 and C-3, the Fe content was found to be 36 wt %, 26 wt % and 17 wt % respectively. Further the result obtained from the EDAX analysis corroborates with the XRD pattern of composites thereby reduction in the peak intensity of Fe₃O₄ (Fig.2 d-f).

3.4. Antibacterial investigation of Ag:HAP-Fe₃O₄-CS hybrid composites

Human pathogens like *E. coli* (gram negative) and *S. aureus* (gram positive) were selected because of their ability to cause common infections in the human body. In this study, all the concentrations of Ag doped HAP (1%, 3% and 5%), Fe₃O₄ and composites of 5%Ag:HAP-Fe₃O₄-CS (C1, C-2 and C-3) were evaluated for their antibacterial activity against the *S. aureus* and *E. coli* organisms. The obtained 0.5 OD cultures of *S. aureus* and *E. coli* were exposed to these individual and composite powders at a concentration of 5 mg/ml and plated onto agar media and allowed to incubate. From Fig. 4, it was observed that all the samples consist of 1%, 3% and 5%Ag:HAP powders were shown good antibacterial activity. The activity was enhanced with increase in the Ag concentration, i.e. 5%Ag:HAP showed excellent activity compared to 1% and 3%Ag:HAP which was found to be completely inhibited the growth of viable *E. coli* and *S. aureus*. However, Fe₃O₄ NPs was also found to shown the significant reduction in the number of colonies when compare with the control of both the pathogens, but *S. aureus* is slightly affected than *E. coli* (Fig. S3). Therefore, based on their antibacterial evaluations of all the powders of Ag doped HAP, 5%Ag:HAP was selected to develop composite with various concentrations of Fe₃O₄ and CS to study the antibacterial behavior.

Further, the prepared C-1, C-2 and C-3 composites were characterized and assessed to resist the growth of microorganisms. It was found that when compared to individual activity of components, the fabricated composites showed an enhanced antibacterial behavior toward *E. coli*, might be due to less denser cell wall. Whereas the results illustrated in Fig. 4, the viable *S. aureus* is somewhat suppressed by the composites and exhibits more colonies than the *E. coli* due to the thick cell wall. The C-2 and C-3 composites have shown complete reduction of *E. coli* than C-1. The C-3 composites have shown higher activity towards *S. aureus* than C-1 and C-2 (Fig. S3). The possible reason behind this scenario is the interaction of released Ag ions from Ag doped HAP, Fe₃O₄ NPs and CS molecules with the membrane of pathogens which is supported by AAS analysis (Fig. S4). These

liberated ions are diffused into the bacterial cell wall and cause the plasmolysis by separation of cytoplasm from bacterial cell wall. Finally, these ions interrupt the replication of DNA strand by demolishing the DNA structure and obstruct the respiration.³⁸⁻⁴¹ This study proves that, the C-1, C-2 and C-3 composites are much efficient in inhibiting the complete growth of common infection causing pathogenic organisms.

3.5. *In vitro* SBF immersion test

Nanocomposite powders (C-1, C-2 and C-3) were immersed in the SBF solution under physiological conditions of pH at 7.35 ± 0.25 for the period of 7 days to determine its bioactive behavior. The bone like apatite layer formation after SBF immersion was shown in the Fig. 5 (a)-(c). As shown in SEM images, the calcium phosphate particles were irregularly deposited on the surface of composites. The rate of apatite formation was found to be more on C-3 composite compared to the other composites, due to the interaction of NH_2 , OH^- groups of CS and PO_4^{3-} group of HAP with Ca^{2+} ions of SBF. This interaction leads to the Ca rich layer on the surface of composites. This surface Ca rich layer will attract the PO_4^{3-} and OH^- ions from SBF solution for the nucleation of apatite layer. The growth of the Ca and P rich layer was lead to the increase of the apatite particle size and raise in the surface roughness in random manner. These nanocomposites exhibit the esteemed bioactive layer formation on their exterior due to increase in the surface area to volume ratio. In order to verify the phase formation, the elements present in SBF soaked composites were examined by EDAX (Fig. 5A (a)-(c)) analysis and confirm the presence of elemental composition as Ca, P, Ag, O, C and Fe. The SBF grown apatite proved as carbonated apatite and was supported by EDAX analysis with presence of carbon atom. These composite materials after SBF treatment have shown the growth of bone like carbonated apatite layer on their surfaces with the increase in the Ca/P ratio as 2.15. Therefore, these nanocomposites can spontaneously make a bond with natural bone through the apatite layer in the *in vivo* applications. The SBF immersed solution was collected and was analyzed by ICP-OES to confirm the leaching of metal ions from composite materials. From this study we observed that the ions such as Ag and Fe are leached out from the composites during immersion periods.

3.6. *In vitro* Hemocompatibility study

In this *in vitro* hemocompatibility assessment, individual components of 5%@Ag:HAP, Fe_3O_4 NPs and composites of 5%@Ag:HAP- Fe_3O_4 with chitosan such as C1, C-2 and C3 were examined with human blood at different concentrations such as 200, 400, 600, 800, and 1000 $\mu\text{g}/\text{ml}$, which can cause the damage to the membrane of blood cells and release of hemoglobin (Fig. S5). According to, ASTM 756-00 and ISO 10 993-5 1992 documents, the hemolytic index range less than 2% is non hemolytic, 2-5% is slightly hemolytic and greater than 5% is hemolytic. From Fig. 6, we observed that 5%@Ag:HAP and Fe_3O_4 are highly hemocompatible with less than 0.9% hemolysis at various concentrations from 200 -1000 $\mu\text{g}/\text{ml}$. The C-1 composite was shown slightly hemolytic when compared with C-2 and C-3 composites with respect to concentrations from 200-1000 $\mu\text{g}/\text{ml}$ which might be due to the penetration of the higher amount of Fe_3O_4 NPs (45%) into the membrane of RBC cells. The electrical charge, surface energy and topography of composite material play significant role in creating adverse effects on erythrocytes and which induce the hemolysis during *in vitro* study.⁴² The C-1, C-2 and C-3 composites are shown the maximum hemolytic ratio as 4.3, 4.25 and 3.7% respectively. The hemolytic ratio of composites specifies that the slight damage of erythrocytes membrane in terms of shrinkage and scrambling, which direct the release of intracellular hemoglobin. However, it

was found that all the composites have shown less than 5% hemolytic activity and proved that these hybrid composites are highly hemocompatible in nature. Thus, this test can be considered as a preface examination of biocompatibility study. This blood compatibility assay proves that the fabricated nanocomposites, acts as favorable materials in clinical applications.

3.7. *In vitro* Biocompatibility study

In vitro biocompatibility assessment was performed on C-3 composite material due to its better inhibition of microorganisms growth by antibacterial activity, less toxic towards the erythrocytes by hemolysis assay and good apatite layer formation on the surface of C-3 in SBF immersion test than C-1 and C-2 composites. This investigation was carried out by MTT assay using NIH-3T3 fibroblast cells for an incubation time of 24 and 48 h at various concentrations such as 200, 400, 600, 800 and 1000 $\mu\text{g}/\text{ml}$. Fig. 7 shows the cell viability of C-3 composite with fibroblast at concentrations of 200-1000 $\mu\text{g}/\text{ml}$, which indicates that control cell viability for 48 h incubation is slightly higher as 105 % than 24 h. The C-3 nanocomposite exhibits marginally minimal cell viability at 200 and 400 $\mu\text{g}/\text{ml}$ as 96 and 94 % respectively for both periods than the controls. The concentrations at 600, 800 and 1000 $\mu\text{g}/\text{ml}$ for the periods of 24-48 h were shown the significant cytotoxicity on the NIH-3T3 fibroblast cells where viability fell as 70, 46 and 34 %, which may be due to leachable of ions from nanocomposite such as Ag and Fe. These results clearly prove that, C-3 composite at 200-400 $\mu\text{g}/\text{ml}$ show better cell attachment, spreading and proliferation than the 600-1000 $\mu\text{g}/\text{ml}$ which is further observed by phase contrast microscopy. The phase contrast micrographs (Fig. 7A) revealed that the NIH-3T3 cell density and response with C-3 composite was excellent at 200-400 $\mu\text{g}/\text{ml}$ than the 600-1000 $\mu\text{g}/\text{ml}$. In these microscopic observations, the adhered viable cells appeared as elongated spindle shaped (green notation) whereas, non viable unadhered cells are found to be in circular shape (red notation).⁴³ Therefore, this study confirms that the fabricated C-3 composite has good cytocompatible with NIH-3T3 cells at lower concentrations to use in biomedical applications.

4. Conclusion

In this present research paper, we have successfully prepared the hybrid composites consist of 5%@Ag:HAP- Fe_3O_4 -CS using the ball milling method.

- Sol-Gel method was employed to synthesize Ag doped Hydroxyapatite with different concentrations of 1%, 3% and 5% Ag content. The XRD diffractogram reveals that there is a slight increase in the lattice parameters upon reduction in the crystallinity with respect to different concentration of silver.
- The hybrid composites of C-1, C-2 and C-3 were made using 5%@Ag:HAP, Fe_3O_4 and CS materials. In FTIR, the peak broadness at $556\text{-}636\text{ cm}^{-1}$ was found to be decreased from C-1 to C-3 due to the lower amount of Fe_3O_4 content which is evidenced by XRD with a decrease in the peak intensity of Fe_3O_4 . The above result was also confirmed by the EDAX study of composite materials, whereas the Fe content was found to be 36 wt %, 26 wt % and 17 wt % respectively.
- Antibacterial activity of the hybrid composites and individual components has showed the greater inhibition efficiency towards *S. aureus* and *E. coli* organisms. The C-3 composites have shown higher activity towards *S. aureus* than C-1 and C-2.
- *In vitro* biomineralization was performed using SBF immersion test and found that the formation of bone

like carbonated apatite on the surface of hybrid composites due to electrostatic interactions of surface ions with SBF solution.

- *In vitro* hemocompatibility test of 5%Ag:HAP, Fe₃O₄ and their composites (C-1 to C-3) proved that all the composites have showed good compatible with human blood. Each composite have shown less than 5% of hemolytic activity and proven that these hybrid composites are highly hemocompatible.
- The study of biocompatibility of C-3 nanocomposite was performed based on antibacterial, hemocompatible activity and SBF immersion study. This *in vitro* study demonstrated that C-3 composite exhibits good cytocompatibility with NIH-3T3 fibroblast cells at the range of concentration from 200 to 400 µg/ml whereas toxic at 600-1000 µg/ml may be due to leaching out of Ag, Fe ions from composite for 24-48 h. The phase contrast images reveal that the prominent activation of cell attachment and proliferation was ensured on the C-3 composite material.

Hence, these *in vitro* biological results suggest that the fabricated multiphase nanocomposites may serves as a potential ceramic material for bone tissue regeneration applications.

Acknowledgments

One of the author U. Vijayalakshmi acknowledges the DST, New Delhi, India (SB/FT/CS-091/2012) for providing financial support. Also the authors express their gratitude to VIT University for rendering all the research facilities. Authors sincerely express their gratitude to Dr. Jabez Osborne W (SBST), Microbial Bioremediation lab for his continuous support in carrying out biological assays.

References

- 1 S. Nayar, M. K. Sinha, D. Basu and A. Sinha, *J. Mater. Sci. Mater. Med.*, 2006, **17**, 1063-1068.
- 2 F. Bakan, O. Lacin and H. Sarac, *Powd. Tech.*, 2013, **233**, 295-302.
- 3 L. Cremet, S. Corvec, P. Bemer, L. Bret, C. Lebrun, B. Lesimple, A. F. Miegerville, A. Reynaud, D. Lepelletier and N. Caroff, *J. Infect.*, 2012, **64**, 169-175.
- 4 N. Iqbal, M. R. A. Kadir, N. A. N. N. Malek, N. H. Mahmood, M. R. Murali and T. Kamarul, *Mater. Lett.*, 2012, **89**, 118-122.
- 5 R. Archana, C. B. Rakesh, N. Duraipandy, M. S. Kiran and K. P. Deepak, *Ceram. Int.*, 2014, **40**, 10831-10838.
- 6 M. Honda, Y. Kawanobe, K. Ishii, T. Konishi, M. Mizumoto, N. Kanzawa, M. Matsumoto and M. Aizawa, *Mater. Sci. Eng. C*, 2013, **33**, 5008-5018.
- 7 L. K. Hye, Y. J. Gil, J. H. Yoon, S. H. Jung, J. P. Yoon, G. K. Do, Z. Miqin and J. K. Dae, *Mater. Sci. Eng. C*, 2015, **54**, 20-25.
- 8 K. Santosh and K. Joonseok, *Int. J. Mol. Sci.*, 2012, **13**, 6102-6116.
- 9 Y. L. Xing, H. N. Kai, S. Shuai and C. Hao, *Int. J. Biol. Macromol.*, 2012, **50**, 43-49.
- 10 L. Kai, S. Hailang, S. Haitao, Z. Yongxing, L. He, W. Xiaofeng and Q. Zhao, *RSC Adv.*, 2015, **5**, 17541-17549.
- 11 H. L. Shih, H. L. Chia, P. B. Bishnu, S. Norihiro, C. Yung, Y. Yusuke, H. L. Feng and C. W. W. Kevin, *Int. J. Nanomedicine.*, 2015, **10**, 3315-3328.
- 12 B. A. Ereath, A. Manmadhan, Y. Yoshiyuki, W. Wilfried and V. Harikrishna, *J. Am. Ceram. Soc.*, 2012, **95**, 2695-2699.
- 13 D. L. Trandafir, C. Mirestean, R. V. F. Turcu, B. Frentiu, D. Eniub and S. Simon, *Ceram. Int.*, 2014, **40**, 11071-11078.
- 14 T. Nhiem and J. W. Thomas, *Acta Biomaterialia*, 2011, **7**, 1298-1306.
- 15 B. Vera and V. Liliana, *Eur. Polym. J.*, 2014, **53**, 171-188.
- 16 C. Huiling, C. Hongpeng, H. Zhanyun and C. Dihu, *Mater. Lett.*, 2014, **124**, 275-278.
- 17 Y. Z. Hui, P. Z. Yan, F. Z. Wei and G. C. Xi, *Carbohydr. Polym.*, 2011, **83**, 1643-1651.
- 18 P. Jongwattanapisan, N. Charoenphandhu, N. Krishnamra, J. Thongbunchoo, I. M. Tang, R. Hoonsawat, S. M. Smith and W. P. On, *Mater. Sci. Eng. C.*, 2011, **31**, 290-299.
- 19 W. Cui, Q. Hu, J. Wu, B. Li and J. Shen, *J. Appl. Polym. Sci.*, 2008, **109**, 2081-2088.
- 20 W. Jia, H. Qiaoling, C. Fuping, L. Baoqiang and S. Jiacong, *Key. Eng. Mat.*, 2007, **330**, 435-438.
- 21 X. ming Pu, K. Wei and Q. qing Zhang, *Mater. Lett.*, 2013, **94**, 169-171.
- 22 L. Pighinelli and M. Kucharska, *Carbohydr. Polym.*, 2013, **93**, 256-262.
- 23 M. Ajeesh, B. F. Francis, John Annie and P. R. Harikrishna Varma, *J. Mater. Sci. Mater. Med.*, 2010, **21**, 1427-1434.
- 24 T. Iwasaki, R. Nakatsuka, K. Murase, H. Takata, H. Nakamura and S. Watano, *Int. J. Mol. Sci.*, 2013, **14**, 9365-9378.
- 25 K. S. Vanka, M. Aparna, S. Sumit and J. O. William, *Research J. Pharm. and Tech.*, 2015, **8**, 167-171.
- 26 T. Kokubo, H. Kushitani, S. Sakka, T. Kitsugi and T. Yamanuro, *J. Biomed. Mater. Res.*, 1990, **24**, 721-734.
- 27 M. Zhifang, B. Jing, W. Yichen and J. Xiue, *Appl. Mater. Interfaces.*, 2014, **6**, 2431-2438.
- 28 S. L. Yu and L. H. Christy, *Chem. Mater.*, 2009, **21**, 3979-3986.
- 29 J. Sushma, D. Ketaki, R. R. Sutapa and K. Meenal, *Appl. Nanosci.*, 2014, **4**, 133-141.
- 30 U. Vijayalakshmi and S. Rajeswari, *J. Sol-Gel. Sci. Technol.*, 2012, **63**, 45-55.
- 31 M. L. P. Paula, P. M. Alexandra, M. P. D. S. Ricardo, P. Iva and L. R. Rui, *J. Mater. Chem.*, 2007, **17**, 4064-4071.
- 32 S. M. Herman, A. P. M. Alexandra, C. Elisabete and V. D. A. Mauro, *J. Mater. Chem. B*, 2013, **1**, 1696-1711.
- 33 C. P. Paula, L. D. S. Ana, S. T. Daniela, M. P. Calatayud, F. G. Gerardo and T. Tito, *Materials*, 2013, **6**, 3213-25.
- 34 S. C. Carmen, L. I. Simona, L. C. Phillippe, V. C. Liliana and P. Daniela, *Res. Lett.*, 2012, **7**, 324.
- 35 S. Vojislav, J. Djordje, D. Suzana, B. T. Sladjana, M. Miodrag, S. P. Mirjana, K. Aleksandra, J. Dragoljub and R. Slavica, *Appl. Surf. Sci.*, 2011, **257**, 4510-4518.
- 36 I. Md Monarul, M. D. M. Shah, M. M. Rahman, I. M. Md Ashraf, A. A. Shaikh and S. K. Roya, *Int. J. Bas. Appl. Sci.*, 2011, **11**, 77-80.
- 37 K. Mahmut, O. Faruk, M. V. Nurhan and E. Mustafa, *Prog. Electromagn. Res.*, 2013, **134**, 509-524.
- 38 H.Y. Song, K.K. Ko, I.H. Oh and B.T. Lee, *Eur. Cell. Mat.*, 2006, **11**, 58.
- 39 M. Vukomanovi, U. Repnik, T. Z. Bergant, R. Kostanjsek, S. D. Skapin, and D. Suvorov, *ACS Biomater. Sci.Eng.*, 10.1021/acsbiomaterials.5b00170.
- 40 K. P. Tank, K. S. Chudasama, V. S. Thaker and M. J. Joshi, *J. Cryst. Growth.*, 2014, **401**, 474-479.
- 41 K. Tank, Scholar's Press, 2014.
- 42 S. Henkelman, G. Rakhorst, J. Blanton, W. V. Oeveren, *Mater. Sci. Eng. C.*, 2009, **29**, 1650-1654.
- 43 U. Anjaneyulu, D. K. Pattanayak and U. Vijayalakshmi, *Mater. Manuf. Process.*, 2006, **31**, 206-216.

Figures and legends

Fig. 1 ATR-FTIR spectroscopy of Chitosan (a), Fe_3O_4 (b), 5%@Ag:HAP (c), C-1 (d), C-2 (e) and C-3 (f).

Fig. 2 Powder-XRD patterns of Chitosan (a), Fe_3O_4 (b), 5%@Ag:HAP (c), C-1 (d), C-2 (e) and C-3 (f).

Fig. 3 SEM images of 5%@Ag:HAP (a), Fe_3O_4 (b), Chitosan (c), C-1 (d), C-2 (e) and C-3 (f).

Fig. 3A EDAX analysis of 5%@Ag:HAP (a), Fe_3O_4 (b), Chitosan (c), C-1 (d), C-2 (e) and C-3 (f).

Fig. 4 Antibacterial activity of 1%, 3% and 5%@Ag:HAP, Fe_3O_4 , C-1, C-2 and C-3 powders against *S.aureus* and *E.coli*.

Fig. 5 SEM analysis of apatite formation on the surface of C-1 (a), C-2 (b) and C-3 (c) composites after immersion in SBF solution for the period of 7 days.

Fig. 5A EDAX analysis of apatite formation on the surface of C-1 (a), C-2 (b) and C-3 (c) composites after immersion in SBF solution for the period of 7 days.

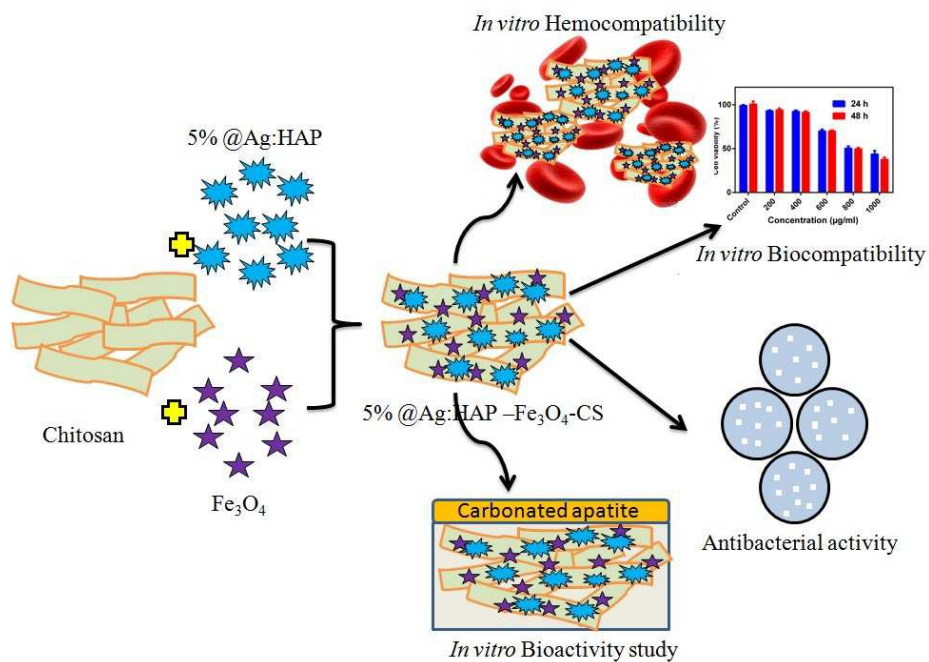
Fig. 6 *In vitro* hemolytic activity of 5%@Ag:HAP, Fe_3O_4 , C-1, C-2 and C-3 materials.

Fig.7 The percentage of cell viability of NIH-3T3 cells on 200-1000 $\mu\text{g/ml}$ concentrations of C-3 nanocomposite for 24-48 h

Fig.7A The cell attachment and proliferation of NIH-3T3 cells on C-3 nanocomposite at the concentrations of 200-1000 $\mu\text{g/ml}$ for 24-48 h. (live cells denoted as green circle and dead cells denoted as red circle).

Tables

Table 1 X-ray diffraction peak positions and miller indices values of Ag doped HAP (1-5%) and Fe_3O_4 NPs.



Graphical abstract of Novel 5% @Ag:HAP-Fe₃O₄-CS hybrid composites and its biological investigations.

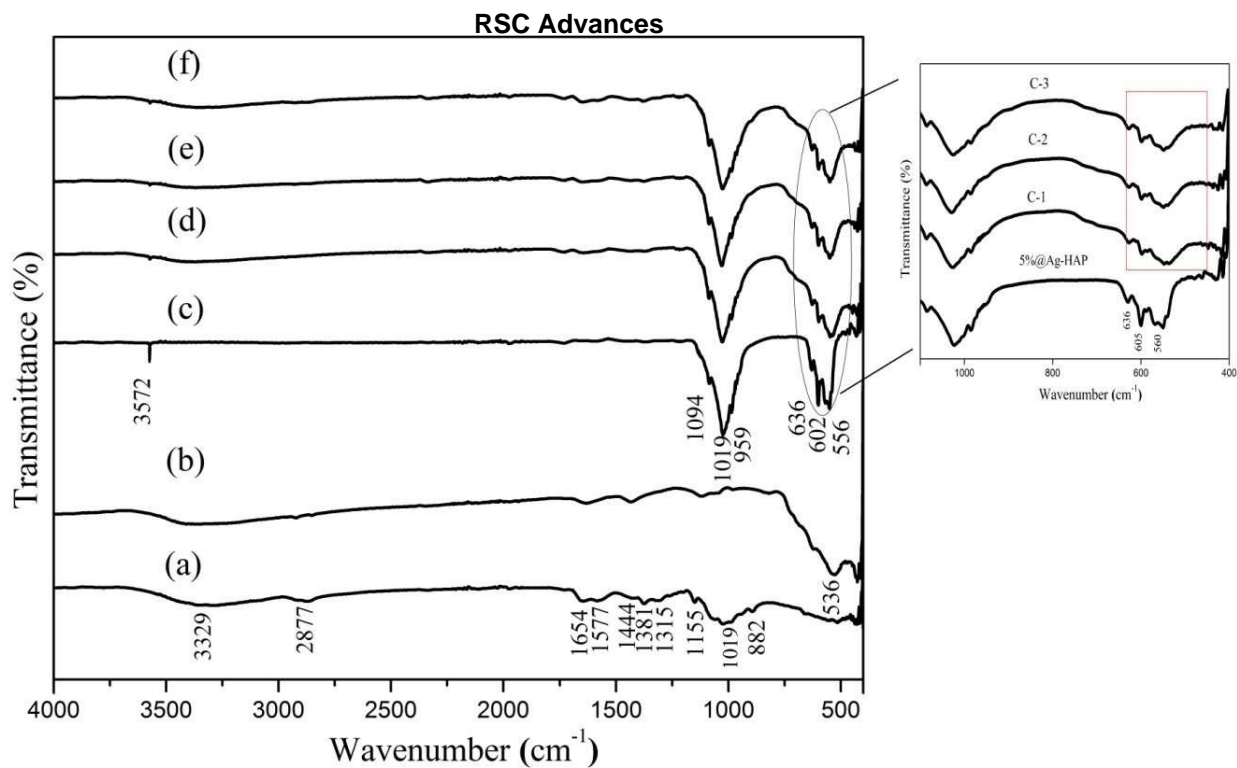


Fig. 1 ATR-FTIR spectroscopy of Chitosan (a), Fe_3O_4 (b), 5%@Ag:HAP (c), C-1 (d), C-2 (e) and C-3 (f).

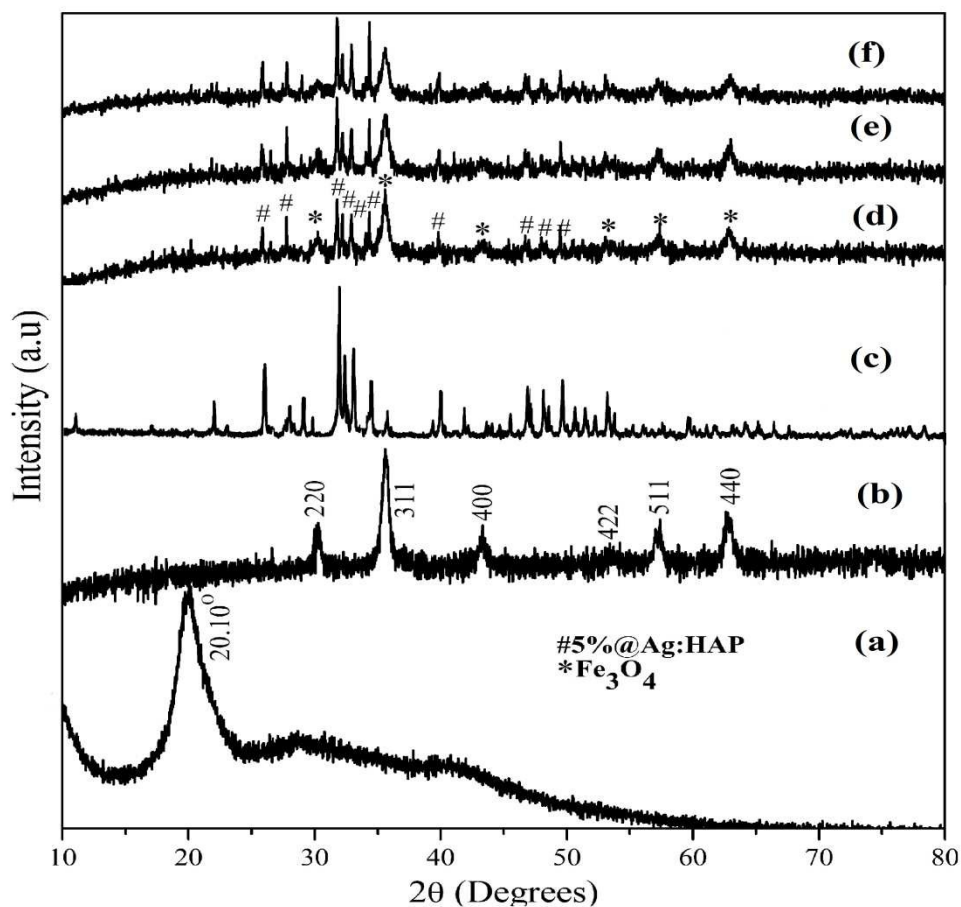


Fig. 2 Powder-XRD patterns of Chitosan (a), Fe_3O_4 (b), 5%@Ag:HAP (c), C-1 (d), C-2 (e) and C-3 (f).

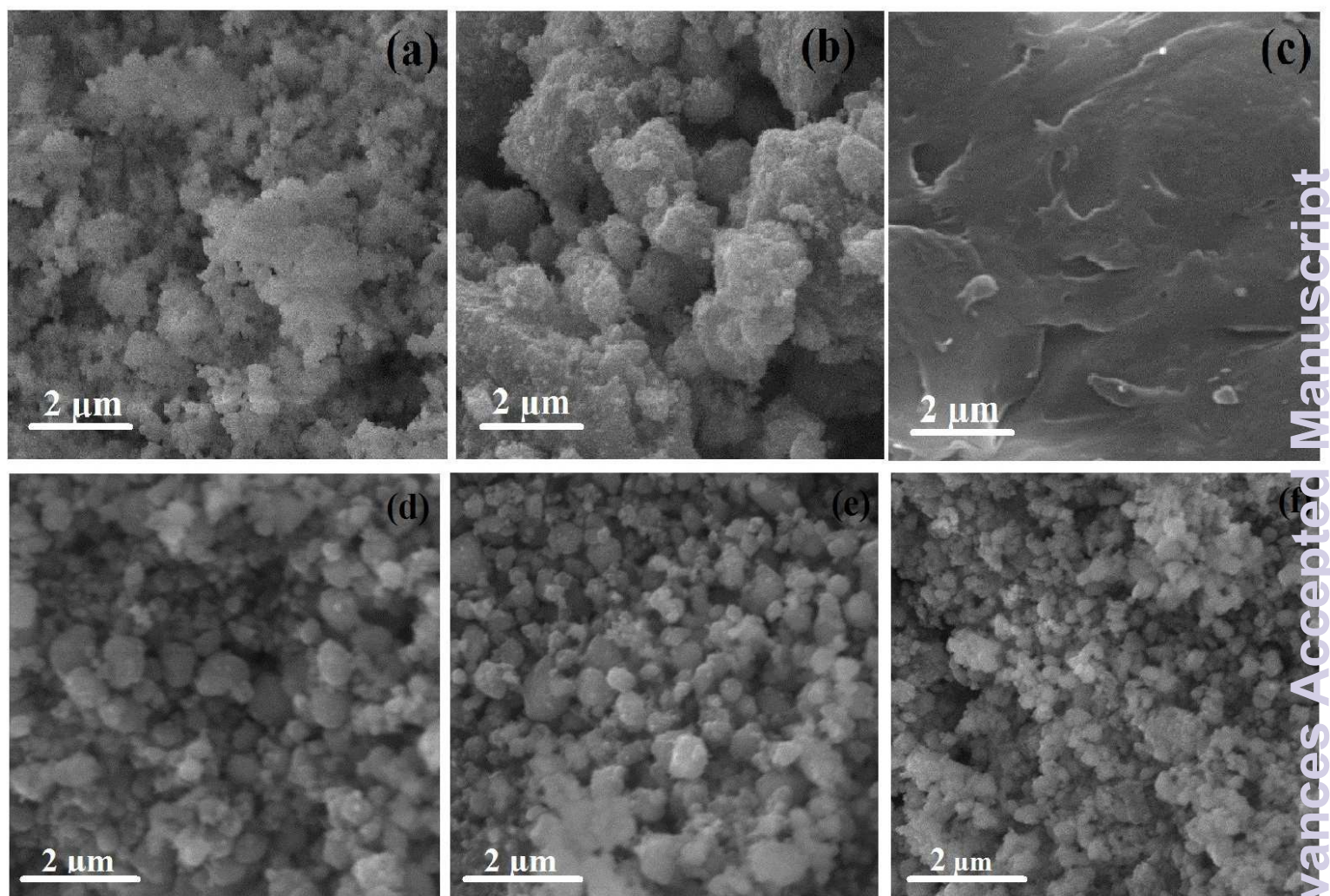


Fig. 3 SEM images of 5%Ag:HAP (a), Fe₃O₄ (b), Chitosan (c), C-1 (d), C-2 (e) and C-3 (f).

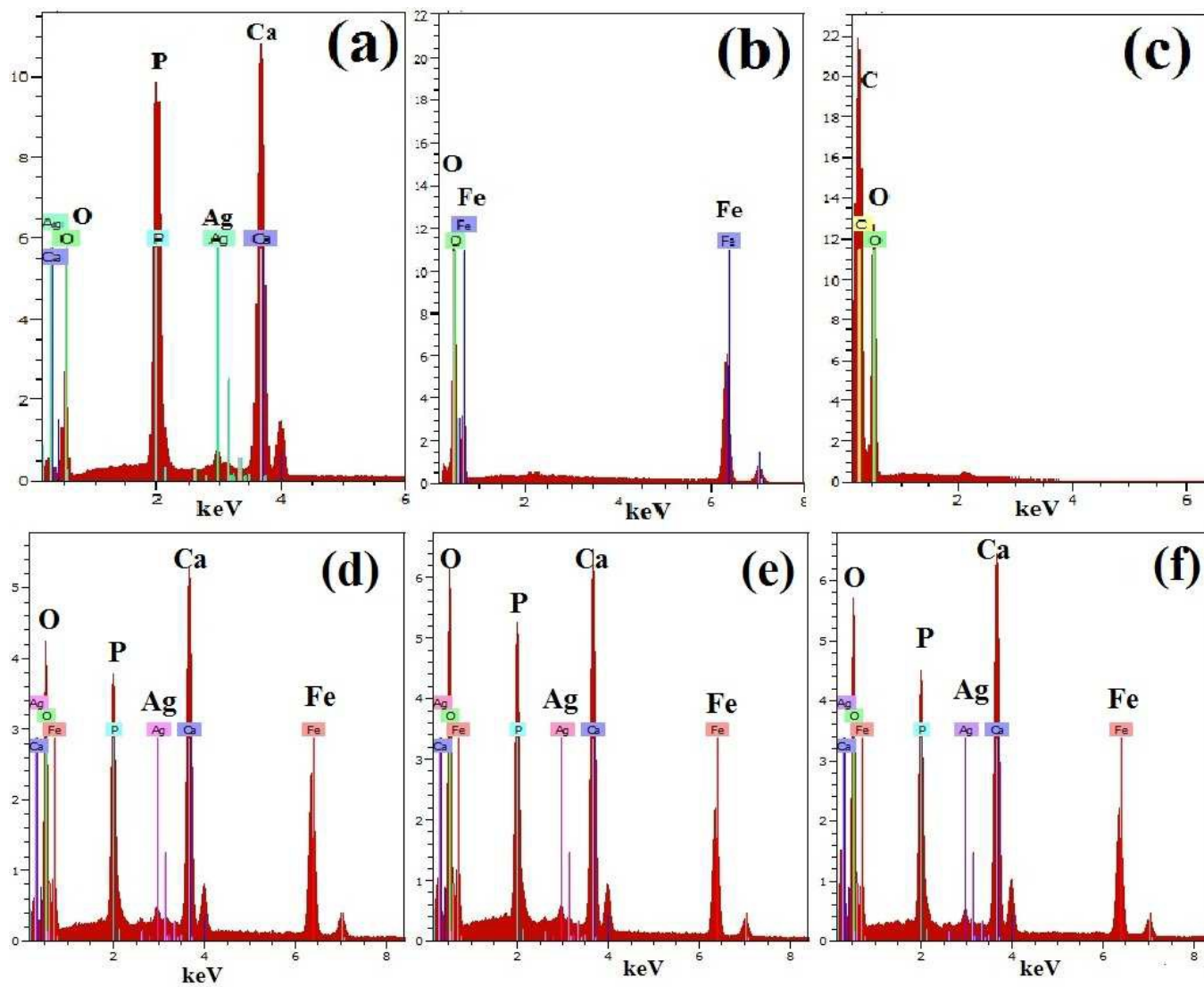


Fig. 3A EDAX analysis of 5% Ag:HAP (a), Fe₃O₄ (b), Chitosan (c), C-1 (d), C-2 (e) and C-3 (f).

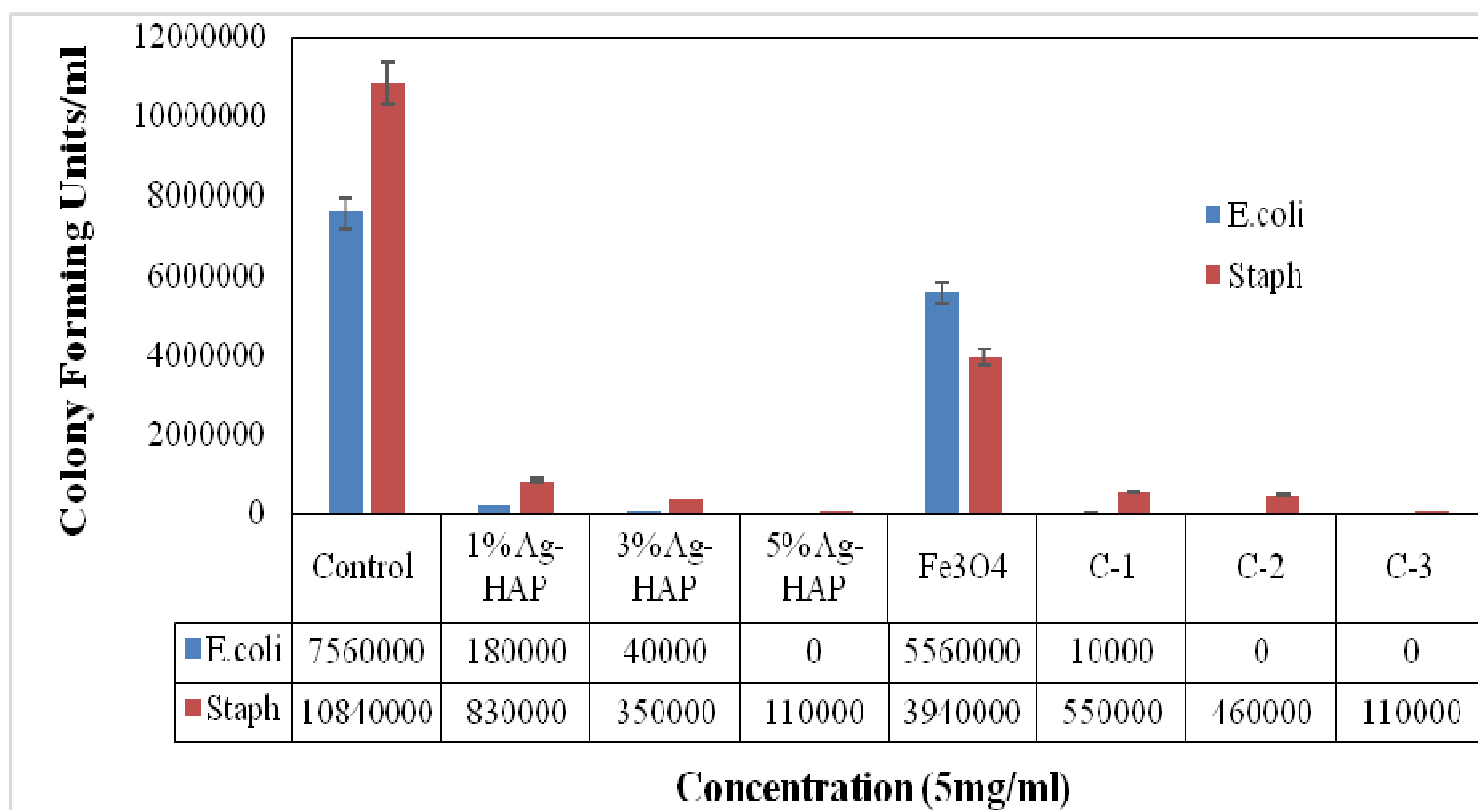


Fig. 4 Antibacterial activity of 1%, 3% and 5%@Ag:HAP, Fe₃O₄, C-1, C-2 and C-3 powders against *S.aureus* and *E.coli*.

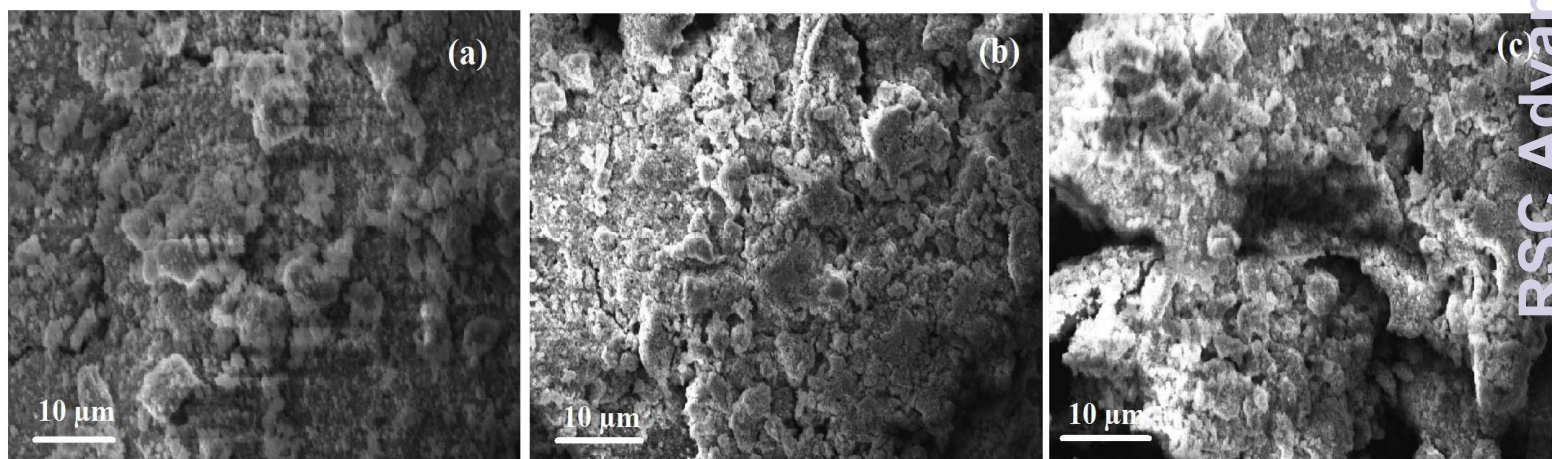


Fig. 5 SEM analysis of apatite formation on the surface of C-1 (a), C-2 (b) and C-3 (c) composites after immersion in SBF solution for the period of 7 days.

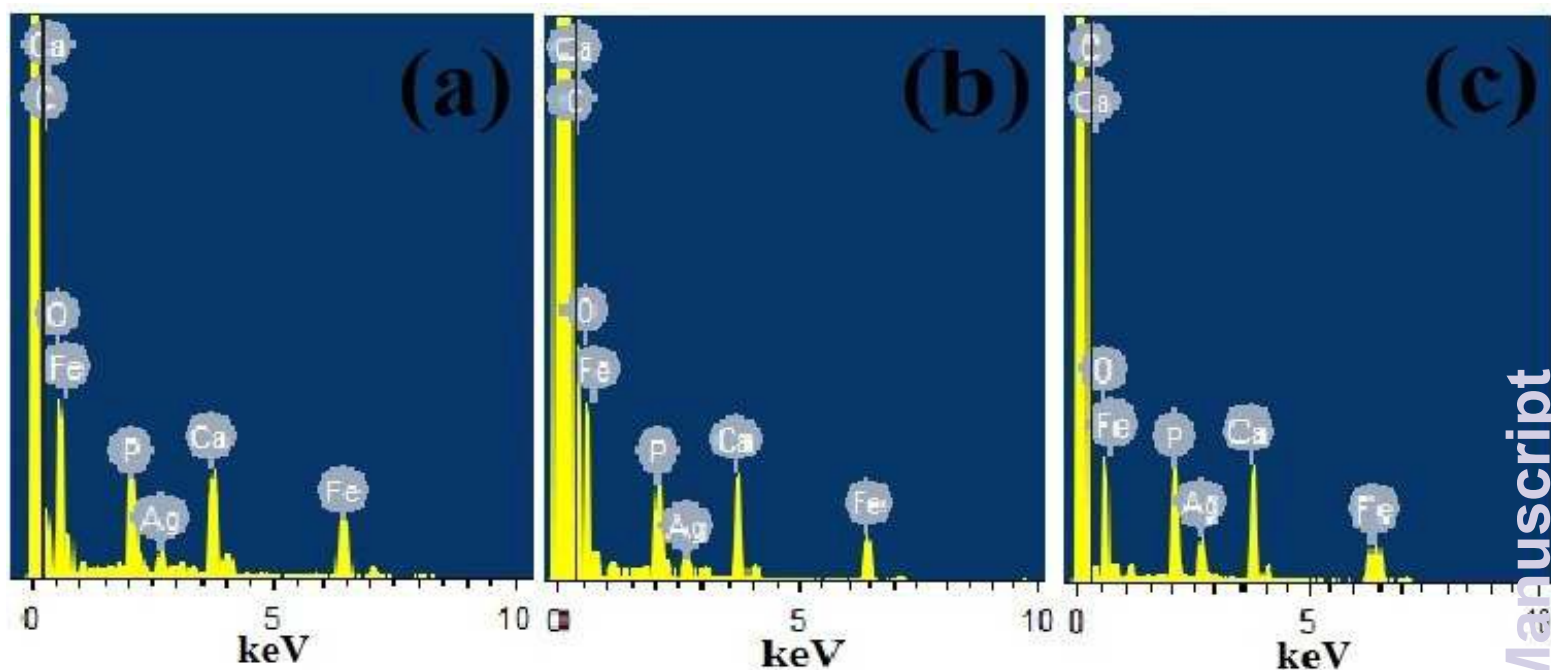


Fig. 5A EDAX analysis of apatite formation on the surface of C-1 (a), C-2 (b) and C-3 (c) composites after immersion in SBF solution for the period of 7 days.

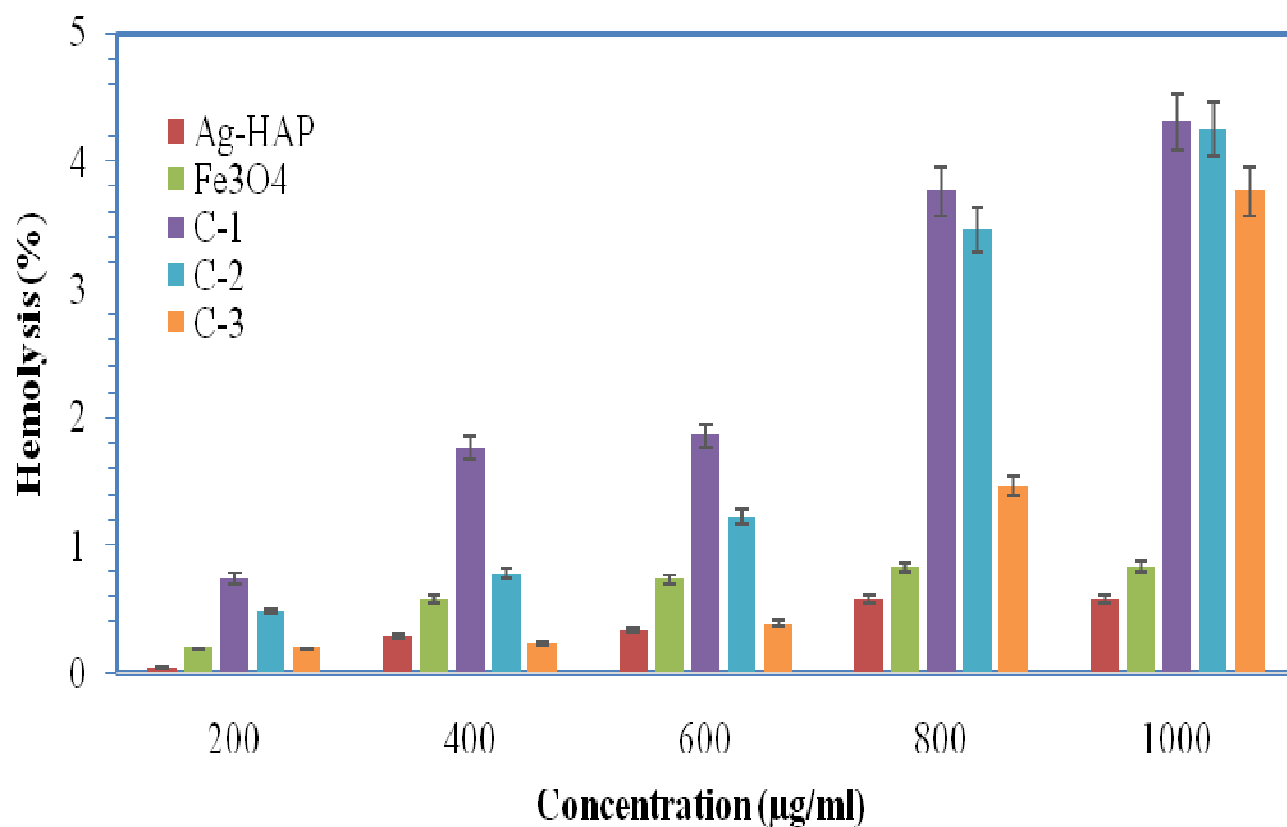


Fig. 6 *In vitro* hemolytic activity of 5%@Ag:HAP, Fe₃O₄, C-1, C-2 and C-3 materials.

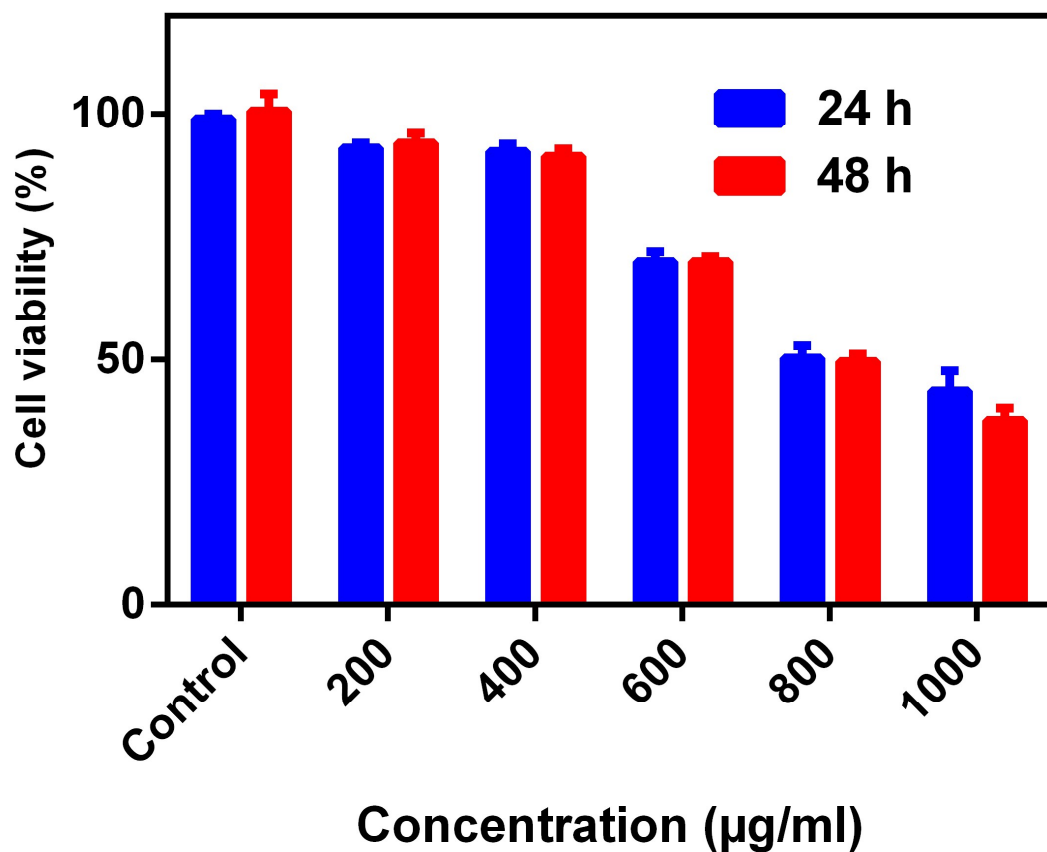


Fig.7 The percentage of cell viability of NIH-3T3 cells on 200-1000 µg/ml concentrations of C-3 nanocomposite for 24-48 h.

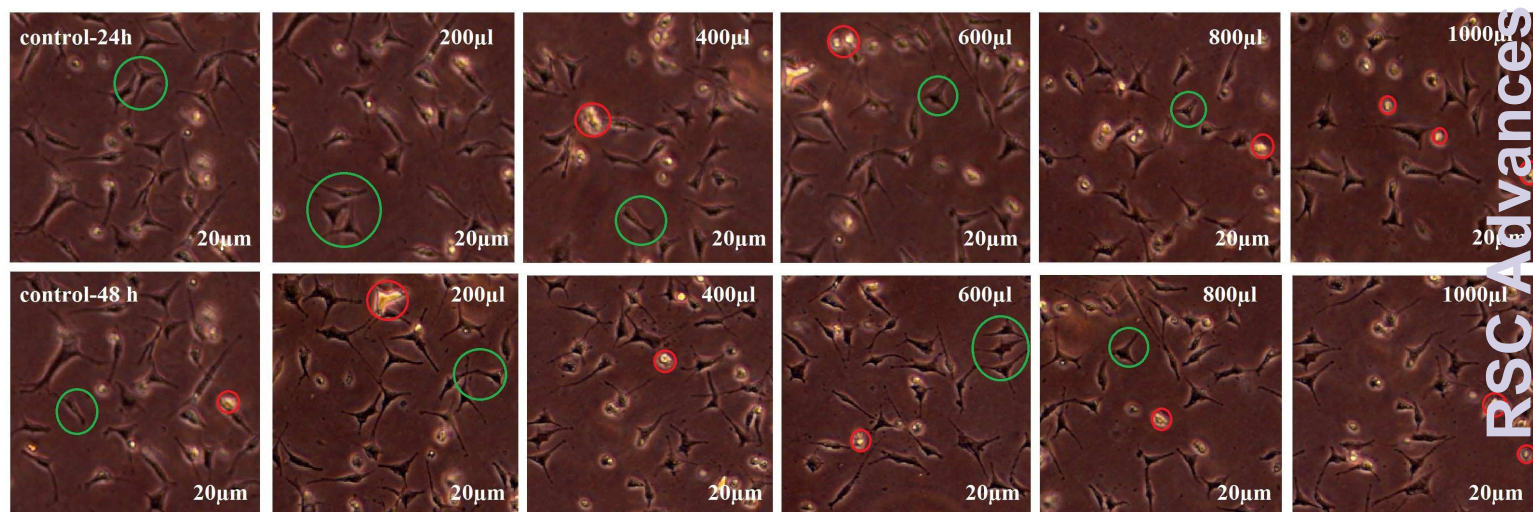


Fig.7A The cell attachment and proliferation of NIH-3T3 cells on C-3 nanocomposite at the concentrations of 200-1000 µg/ml for 24-48 h (live cells denoted as green circle and dead cells denoted as red circle).

Table 1 X-ray diffraction peak positions and miller indices values of Ag doped HAP (1-5%) and Fe₃O₄ NPs.

S.No	Ag doped HAP (1%, 3% & 5%)		Fe ₃ O ₄ NPs	
	2 Theta (Degrees)	hkl	2 Theta (Degrees)	hkl
1	25.75	(002)	30.21	(220)
2	28.09	(102)	35.69	(311)
3	28.99	(210)	43.44	(400)
4	31.87	(211)	53.40	(422)
5	32.33	(112)	57.25	(511)
6	32.95	(300)	62.82	(440)
7	34.02	(202)		